Title

Interaction of myoglobin with oleic acid

Authors

Shih, Lifan
Chung, Youngran
Sriram, Renuka
et al.

Publication Date

2015-10-01

DOI

10.1016/j.chemphyslip.2015.07.010

Peer reviewed

HHS Public Access

Author manuscript

Chem Phys Lipids. Author manuscript; available in PMC 2016 October 01.

Published in final edited form as:

Chem Phys Lipids. 2015 October ; 191: 115–122. doi:10.1016/j.chemphyslip.2015.07.010.

Interaction of Myoglobin with Oleic Acid

Lifan Shih, **Youngran Chung**, **Renuka Sriram**, and **Thomas Jue**

Department of Biochemistry and Molecular Medicine, University of California Davis, Davis, CA 95616-8635

Abstract

Previous studies have shown that palmitate (PA) can interact with myoglobin (Mb). The present study has investigated the interaction of the more soluble unsaturated fatty acid, oleic acid (OA). Indeed, ^{1}H NMR measurements of the Mb signal during OA titration also show signal changes consistent with specific and non-specific binding. At OA:Mb ratio < 4:1, OA perturbs selectively the 8-heme methyl signal, consistent with a local and specific fatty acid-protein interaction. As OA:Mb ratio increases from 4:1 to 40:1, all hyperfine shifted MbCN signals decrease, consistent with a non-selective, global perturbation of the protein. The pH titration analysis indicates that the observed OA methylene signal in the presence of Mb reflects a non-specific interaction and does not originate from a shift in the lamella-micelle equilibrium. Given the OA interaction with Mb, a fatty acid flux model suggests that Mb can play a fatty acid transport role under certain physiological conditions.

Keywords

Lipid; lipid-protein interaction; fatty acid; NMR; metabolism; bioenergetics

1. INTRODUCTION

Even though biochemistry canon asserts an O_2 storage and a facilitated O_2 transport role for Mb, many questions still abound about its cellular function (21; 55; 56). Experiments have certainly detected Mb supplying O_2 in plants and in mammalian tissue, and *in vivo* NMR experiments have observed Mb releasing its O_2 store to maintain oxidative metabolism during apnea and at the initiation of skeletal muscle contraction (5; 42). Yet, under anoxia the O_2 store of Mb in mammalian heart can only prolong normal respiration for only a few seconds (4). CO inactivation of Mb function does not impair cardiac respiration, metabolism or contraction (3; 14). Indeed, a mouse without Mb exhibits no striking deficits in its oxygen consumption rate, contractile function, bioenergetics, and metabolism (13; 19). Despite

Correspondence: Dr. Thomas Jue, Biochemistry and Molecular Medicine, University of California Davis, Davis, CA 95616-8635, Phone: (530) 752-4569, FAX: (530) 752-3516, TJue@ucdavis.edu.

Conflict of Interest

The authors have no conflict of interest.

compensating physiological mechanisms, the knock-out (KO) mice have led to suppositions about a nitric oxide (NO) bioscavenging and NO reduction role for Mb (11; 28; 30; 43).

In the Mb KO myocardium, metabolism switches its substrate preference from fatty acid (FA) to glucose. FA to glucose utilization ratio drops from 3/1 to 0.7/1 (10). Many researchers have simply ascribed the metabolic switch to the missing contribution of Mb in facilitating O_2 transport, since oxidative fatty acid metabolism requires O_2. However, several studies have now shown that Mb in the cell appears to diffuse too slowly to compete effectively with free O_2 (33; 34; 40; 41). If Mb does not have a predominant storage or facilitated diffusion O_2 under normal physiological conditions, the reduced fatty acid metabolism could indicate a missing Mb mediated fatty acid transport, as some early Mb studies have implicated (17; 18; 20).

Indeed, recent ^{1}H NMR studies have found evidence for palmitate (PA) binding specifically and non-specifically with Fe (III) MbCN (48). Moreover, PA interacts differentially with physiological states of Mb. PA interacts with MbCO but does not interact with deoxy Mb. The results suggest that Mb could serve as a fatty acid transporter and use a convenient loading-unloading mechanism that follows the O_2 gradient from the sarcolemma to the mitochondria. In fact, a fatty acid transport model indicates that Mb can compete effectively with fatty acid binding protein (FABP) above a fatty acid concentration threshold (47).

To corroborate and characterize the fatty acid interaction with Mb, we have conducted a set of experiments with oleic acid (OA), an 18 carbon (C18) unsaturated fatty acid. Because OA has a higher solubility than PA, it permits the use of a wider range of fatty acid concentrations to titrate into Mb. As with PA, OA interacts specifically and non-specifically with MbCN to perturb selectively the 8-heme methyl signal (32). At high OA:Mb, OA perturbs the overall Mb structure.

The experimental results confirm that Mb can interact specifically and non-specifically with OA without forming a detectable amount of hemichrome. Moreover, the Mb interaction with OA does not appear to arise from any alteration in the lamella-micelle equilibrium. Given the specific interaction of OA, a model of intracellular fatty acid transport indicates that Mb can compete with fatty acid binding protein (FABP) to transport both saturated and unsaturated fatty acid in the cell (16; 33; 34; 47; 48). Mb may then have a role in regulating fatty acid metabolism and presents a unique model to interrogate protein-fatty acid interaction.

2. EXPERIMENTAL

2.1. Protein Preparation

Mb and albumin solutions were prepared from lyophilized horse heart protein and essentially fatty acid free bovine serum albumin (Sigma Chemical Inc., St. Louis, MO). DeoxyMb was prepared from lyophilized metMb as described previously (29). The preparation of MbCO solution followed a similar procedure. All the samples were prepared in 30mM Tris buffer with 1mM EDTA at pH 7.4. The pH was measured at 35ºC using a calomel electrode (Orion 7110BN Micro Calomel pH, Thermo Electron Corporation). Five

times excess KCN was added to the metmyoglobin in Tris to produce MbCN, and the pH was adjusted to 7.4.

A UVIKON (941KONTRON Instruments) spectrophotometer measured the MbCN absorbance from 300-650 nm. Specifically, extinction coefficient of the 542nm absorbance ($\varepsilon 542=11.3 mM^{-1}\cdot cm^{-1}$) provided the basis to determine the MbCN concentration.

2.2. Fatty Acid-Mb Preparation

OA (Sigma Chemical Inc., St. Louis, MO) and $^{13}C_1$ OA (Cambridge Isotope, Tewksbury, MA) were dissolved in 30mM Tris buffer with 1mM EDTA at pH 8.5 at 65ºC. Stock solutions of 10mM and 100mM were prepared and kept in a heating block (Thermolyne 17600 Dri-Bath) at 65ºC. An aliquot of 10mM or 100 mM OA in Tris buffer at 65ºC was added to 600μl of 0.2-0.8 mM myoglobin at 35ºC to yield a final solution with Mb:OA ratios from 1:0.1 to 1:60. In these experiments, the methodological approach appears more effective and efficient than the alternative procedure that requires first dissolving a fatty acid solution in the NMR tube, evaporating the organic solvent, and then adding stoichiometric amount of protein to create the final fatty acid: protein mixture (7).

The time between OA addition and the start of the NMR measurement was approximately 5 minutes. The pH was measured at 35ºC using a calomel electrode. All NMR experiments were then conducted at 35ºC.

2.3. NMR

A Bruker Avance 600 MHz spectrometer recorded the ^1H NMR signals. The 5 mm probe ^1H 90° pulse, calibrated against the HOD signal from a 0.15 M NaCl solution, was 9 μs. Watergate pulse sequence was used to suppress the water signal. Sodium-3-(trimethylsilyl) propionate 2,2,3,3 d4 (TSP) served as the internal chemical shift and concentration reference. All samples contained 10% D_2O to enable the deuterium lock during signal acquisition. All measurements were carried out at 35ºC. A typical spectrum required 1024 scans and used the following signal acquisition parameters: 36 KHz spectral width, 8k data points, and 124ms recycle time.

The ^{13}C signals collected at 151 MHz used the following acquisition parameters: 8.25 μs 90 pulse, a 33 KHz spectral window, and 16K data point and 1.25s recycle time. A GARP pulse sequence decoupled the ^1H signals, and $^{13}C_2$ acetate provided an internal chemical shift reference at 24.2 ppm. Zero-filling the free induction decay (FID) and apodizing with an exponential window function improved the spectra. A spline fit then smoothed the baseline.

2.4. PK Determination

NMR determination of pK used the following equation that relates the observed chemical shift to pH and pKa:

$$\delta_{\text{observed}} = \delta_{\text{p}} + \frac{\delta_{\text{d}} - \delta_{\text{p}}}{1+10^{[\text{pKa}-\text{pH}]}}$$

$\delta_{observed}$ = observed chemical shift at a given pH, δ_p=chemical shift of the protonated form, δ_d=chemical shift of the deprotonated form.

2.5. Fatty Acid Binding Affinity

The curve fit used the equation $[OA]_{bound} = \frac{B_{1max}[OA]}{K_{d1}+[OA]}$ to determine a one site specific binding of OA to Mb based on the signal intensity loss of the 8 heme methyl where OA:Mb < 2:1.

[OA] = oleate; K_d = dissociation constant; and B_{max}= maximum capacity for oleate binding. The analysis assumes that the maximum signal loss of the 8-heme methyl corresponds to B_{1max} or the fully OA bound state.

Modeling a 2-site binding (a specific and a non-specific binding site) used the following equation:

$$[OA]_{bound} = \frac{B_{1max}[OA]}{K_{d1}+[OA]} + \frac{B_{2max}[OA]}{K_{d2}} = \frac{B_{1max}[OA]}{K_{d1}+[OA]} + Ns[OA]$$

At high OA concentration, the analysis assumes Ns= B_{1max}/K_{d1} in the region where $K_{d2} \ll$ [OA] (37).

2.6. Intracellular Fatty Acid Transport

The intracellular fatty acid flux has contributions from free OA and protein mediated OA diffusion as expressed in the following equation, which assumes zero unbound OA at the mitochondrial surface:

$$J = D_{OA}OA + D_X C_X \frac{OA}{K_D^X + OA}$$

J=the overall fatty acid flux, OA=oleic acid; C_X = cellular concentration of Mb ($[Mb]_{cell}$) or FABP ($[FABP]_{cell}$); D_{OA}=diffusion coefficient of free oleic acid, D_X = diffusion coefficient of Mb (D_{Mb}) or FABP (D_{FABP}) in the cell, K_D^X = *in vitro* OA dissociation constant of Mb or FABP (33-35; 44; 48). Because the reported diffusion coefficients of fatty acid in the cell vary widely from 3.5×10^{-9} cm^2s^{-1} to 4.6×10^{-6} cm^2s^{-1}, the model has used the highest value to set an upper bound for unbound OA contribution (35; 52). The model also assumes an identical *in vitro* and *in vivo* K_D^X. Table

2.7. Statistical Analysis

Statistical analysis used the Sigma Plot/ Sigma Stat program (Systat Software, Inc., Point Richmond, CA) and expressed the data as mean value ± standard error (SE). Nonlinear regression analysis of the average data points determined the dissociation constant using Marquardt-Levenberg algorithm. Statistical significance was determined by two-tailed student's t-test, $P<0.05$.

3. RESULTS

The addition of OA to MbCN produces a selective signal intensity loss of the 8 heme methyl resonance (inset figure of heme). Figure 1 shows the 10-30 ppm spectral region of 0.8mM MbCN with and without at a 1:1 ratio of OA:Mb in Tris and in phosphate buffer (Pi) at pH 7.4 and 35ºC. The ^{1}H NMR MbCN spectra with OA in Tris (fig 1A-1B) and Pi (fig 1C-1D) show a selective signal intensity decrease of 8 heme methyl peak at 13.2 ppm, fig. 1. Neither the hyperfine shifted heme 5-CH_3 (26.2 ppm) nor 1-CH_3 (17.8 ppm) peak shows any significant perturbation (2; 32).

Given the selective change of the 8 heme methyl signal and an apparent signal intensity plateau at about OA:Mb 2:1, which the data analysis has presumed to correspond to a fully OA bound Mb (Mb-OA) state, a graph of the fractional amount of Mb-OA as a function of OA leads to the determination of an apparent K_d = 45 μM for the specific OA binding to MbCN, fig 2 (47; 48).

At high OA:Mb ratios (8:1 to 40:1), however, all the hyperfine shifted signals (10-30 ppm) of MbCN lose intensity. New peaks around 8-9 ppm emerge, fig 3. Above an OA:Mb ratio of 24, all hyperfine shifted signal intensities approach zero.

Fig 4 graphs the peak intensity of the heme 1-CH_3 and 8-CH_3 as a function of added OA. The heme 8-CH_3 peak intensity decreases selectively to about 0.6 of its original intensity as OA:Mb reaches 2:1. Continuing addition of OA decreases intensity of all observed hyperfine shifted signals. Above an OA:Mb ratio of 2:1, the 1-CH_3, 5-CH_3, and 8-CH_3 signal intensities begin to decrease similarly with respect to OA (1-CH_3: $y = -0.032x + 0.96$ ($r=0.99$); 5-CH_3: $y = -0.032x + 0.96$ ($r=0.99$); 8-CH_3 : $y = -0.029x + 0.70$ ($r=0.99$)). The 5-CH_3 and 1-CH_3 signal intensities show an identical relationship with OA (5-CH_3 data not shown). The 8-CH_3 peak intensity drops selectively at OA:Mb < 2:1. Above OA:Mb of 2:1, its signal intensity loss parallels the response of the 5-CH_3 and 1-CH_3 signal to OA.

Despite the large alterations in the NMR spectra with high OA:Mb ratios, the characteristic Mb Soret band at 422 nm shows no significant perturbation with OA:Mb ratio up to 5:1. From OA:Mb ratios between 20:1 to 50:1, the band shifts slightly to 420 nm and exhibits < 5% reduction in intensity, fig 1S (Supplemental Data). The optical spectra show no detectable metMb signal.

The chemical shift of the EFG peak in the ^{1}H NMR spectra of OA does not respond to pH change. In either Tris at pH 7.4 or Tris at 12.1, the EFG peak position remains constant. Fig 5A and 5B show the ^{1}H NMR OA spectra in Mb and in Tris buffer at pH 7.4 and pH 12.1, respectively. The EFG peak of OA in Tris and Pi appears at 1.32 ppm.

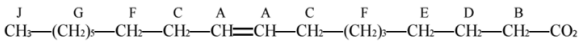

In Mb, the EFG peak position shifts upfield 0.13 ppm to 1.19 ppm, fig 6C. OA in Pi yields a similar spectral profile (data not shown). Peaks B and C also show a slight 0.07ppm upfield shift and peak J show a 0.02 ppm during the transition from pH 7.4 to 12. Peak C shifts 0.23

ppm upfield, while peak J shifts 0.11 ppm. The peak line widths vary with pH and in the presence of Mb, Table 1-2.

The EFG signal of OA yields an estimate of OA solubility in Tris, in Pi, and in Mb. NMR detects about 43% of the OA in Tris or inorganic phosphate (Pi) but about 78% of the OA in Mb, Table 3.

Fig 6 and 7 show the pH dependent change of the various OA peaks in the ^{1}H NMR spectra. The pH dependent chemical shift for peaks B and D, referenced to peak position at pH 12.14, yields a pK of 8.22 and 8.07, respectively, fig 6. In contrast, peaks C, EFG, and J, referenced to the respective chemical shifts at pH 2, exhibit a pK of 5.37, 5.40, and 5.76, respectively, fig 7 and Table 4.

The ^{1}H NMR chemical shifts of OA in Mb do not match the OA peak positions in the monomer, lamella, or micelle state below the critical micelle concentration (CMC), Table 5.

$^{13}C_1$ chemical shift of OA in Tris also varies with pH, fig 8. Below pH 6, it appears at 180.6 ppm. Above pH 9, it resonates at 184.0 ppm. Analysis of the pH titration curve yields a pK=8.42. At pH 7.4 the $^{13}C_1$ OA peak appears in Tris at 180.9 and in Mb at 181.3 ppm, fig 2S (Supplemental Data).

The experimentally determined Mb-OA K_d of 45 μM provides an input value for a model of intracellular fatty acid flux, given the assumption that MbCN and MbO_2 exhibit similar Kd values, fig 9, Table 6, and equation 1 (47; 48). Curve A estimates the FABP mediated fatty acid flux using a cellular FABP concentration of 50 μM and a K_d = 14 nM (15; 45). Literature reports provide the diffusion coefficients for FABP (D_{FABP}) and Mb (D_{Mb}) (34; 35). Curve B shows fatty acid transport based OA solubility and diffusion coefficient of free OA in Tris. Curve C shows that Mb facilitated transport of OA based on cellular concentration of [Mb]=0.26mM and the apparent K_d=45μM will exceed FABP facilitated OA flux at cellular OA concentration above 0.02μM (36; 48). OA in the presence Tris (43% solubility) will exceed FABP facilitated OA transport at 0.07 μM OA.

4. Discussion

4.1. Specific OA Interaction with Mb

Previous experiments have shown that the addition of palmitate (PA) to Fe (III) MbCN perturbs selectively the hyperfine shifted 8 heme methyl signal. Mb also increases the PA solubility (47; 48). However, PA does not interact specifically or non-specifically with deoxy Mb. The contrasting PA interactions with ligated vs. unligated Mb have spawned a hypothesis that Mb could play a potential role in transporting intracellular fatty acid. The differential fatty acid binding affinity with the state of Mb oxygenation provides a convenient mechanism for loading and unloading fatty acid. At the sarcolemma, the high oxygen environment favors MbO_2 and fatty acid binding, while at the mitochondria, the low O_2 environment favors deoxy Mb and fatty acid release.

Whether Mb binds only to PA or can bind other fatty acids, such as OA, poses a fundamental question. OA has a different molecular conformation, because of the

unsaturated bond between carbons 9 and 10 and has a higher solubility than PA in aqueous solution.

Indeed, Mb can bind OA specifically and non-specifically. The interaction does not depend on any special property of Tris buffer. It also occurs in standard Pi buffer. As in the case with PA, the addition of OA produces a selective intensity loss of the distinct hyperfine shifted signal of the 8-heme methyl group in the ^{1}H NMR spectra of MbCN. The analysis of the 8-heme methyl signal vs. OA titration curve leads to the determination of an apparent K_d = 45μM, a value similar to the MbCO-PA Kd = 39-48μM and the MbCN-PA K_d =43μM (47; 48).

4.2. Non-specific interaction of OA with MbCN

Comparative NMR analysis of $^{13}C_1$ OA in buffer and in Mb solution provides perspectives on the Mb and OA interaction. The $^{13}C_1$ OA signal appears at 181.3 ppm in the presence of Mb and grows as OA concentration increases. The $^{13}C_1$ OA chemical shift in Mb also deviates from its corresponding position in Tris buffer at pH 7.47 (180.9 ppm) and at pH 12.14 (184.0 ppm). Since fatty acid exists predominantly in either a lamellar-aqueous phase at pH 7 or a micellar-aqueous phase at pH 12, a plot of the chemical shift $^{13}C_1$ OA signal in Tris buffer as a function of pH reveals an apparent pK = 8.42, consistent with literature reports (8). From this perspective, the position of C_1 OA in Mb (181.6 ppm) could indicate an alteration of the lamella-micelle equilibrium, which gives rise to the observed shift in the ^{1}H NMR OA signals in Mb.

However, the ^{1}H NMR data of OA in buffer at different pH values and in Mb solution provide no corroborating evidence. In buffer, the transition of OA from pH 7.4 to 12.1 does not produce a shift in the EFG peak. Peaks B and C show a slight 0.07ppm upfield shift, while peak J exhibits a 0.02 ppm shift. In Mb, peak C shifts upfield 0.23 ppm; peak J, 0.11 ppm; and peak EFG, 0.13 ppm (8). A similar 0.1 ppm upfield shift of the PA $–CH_2$ shift accompanies the interaction of PA with Mb (47; 48). The ^{1}H NMR OA peaks in the presence of Mb at pH 7.4 do not approach the OA chemical shifts of either the lamella or micelle state observed at pH 7.4 and 12.1, respectively. Consequently, the spectral changes observed in the interaction of OA with Mb do not correspond to simply a shift in the lamella to micelle equilibrium in fatty acid concentration well below the CMC (47; 48).

However, additional work must characterize thoroughly the fatty acid phases during OA titration, following the approach reported previously (6).

4.3. OA Solubility in Mb

The NMR visible $–CH_2$ OA signal (EFG) reflects the soluble OA fraction, since NMR cannot detect large lamellar complexes of OA or OA precipitate, which would yield severely broadened signals (48). Based on the EFG signal, about 43% of the total OA appears soluble in Tris buffer at pH 7.4 but 78% appears soluble in Mb at pH 7.4. In contrast, only 0.8% of PA appears soluble in Tris but 31% appears soluble in Mb (48).

4.4. OA interaction at high OA:Mb ratios

The supposition of a specific interaction of fatty acid with Mb predicates on a selective change in the 8 heme methyl at OA:Mb ratio below 4:1. The 5-methyl, 1-methyl, and other hyperfine shifted signals do not exhibit any significant change. However, above OA:Mb ratio 4:1, all hyperfine shifted resonances begin to lose their respective signal intensity. New peaks around 8 ppm emerge. These signals do not arise from oleic acid. At OA:Mb ratio 40:1, all the paramagnetic shifted peaks of Mb have disappeared.

Given a 2-site ligand binding model, a plot of the 1, 8 heme methyl signal from low to high ratio of OA:Mb yields a biphasic curve. At low OA:Mb, the OA dependent changes in the 8-methyl signal yield an apparent K_{d1} =45 μM (47; 48). At high OA:Mb ratios, the 8-methyl signal yield a weaker dissociation constant of K_{d2}=37 mM. The observation agrees with the interpretation of a specific and non-specific binding of OA to Mb.

Because the heme electronic structure of low spin Fe (III) MbCN, which responds to the alteration in the heme environment, determines the unique heme group hyperfine shift and signal intensity, the non-selective change in the ^{1}H NMR spectra of MbCN upon the addition of high ratio of OA:Mb up to 40:1 indicates a significant structural perturbation of the heme pocket (31).

Despite the substantial OA induced perturbation of Mb in the NMR spectra, the optical spectra do not show a significant change from OA:Mb of 5:1 to 50:1. At OA:Mb of 50:1, the visible Soret band shifts from 422 to 420 nm and exhibits only a 5% reduction in intensity. In contrast, a 25:1 ratio of sodium dodecyl sulfate (SDS) to Mb will shift the Soret band by 5 nm and lose 25% of its signal intensity (50). Moreover, the optical spectra do not detect any signs of hemichrome formation as previously reported at high ratios of fatty acid to hemoglobin (Hb) (1; 39).

4.5. Implication for Intracellular Fatty Acid Transport

Given the literature reported values for FABP (K_d, D_{FABP}, $[FABP]_{cell}$) and Mb (D_{Mb}, $[Mb]_{cell}$), the Mb Kd for OA and the OA solubility determined in the present study provide input parameters to model fatty acid transport in the cell. At low [OA] (below 0.02 μM) FABP mediated transport will predominate. Above 0.02 μM OA, however, Mb begins to dominate. The cross over point depends on relative Kd but also on D_{FABP}/D_{Mb} and $[FABP]_{cell}/[Mb]_{cell}$. Even though free fatty acid has a higher diffusion coefficient than either D_{FABP} or D_{Mb}, its limited solubility reduces its overall contribution to the fatty acid flux. Nevertheless, OA can provide significant contribution, when the cellular concentration reaches 0.03-0.07 μM.

Many questions still surround the model, which attempts to delineate the contribution of FABP, Mb, and free fatty acid to fatty acid transport and metabolism. Even though experiments have partitioned the Kd for Mb vs bovine serum albumin (BSA), no experiments have yet determined the relative Kd for Mb and FABP (47). Nevertheless, the model suggests that Mb can compete with Mb above a threshold fatty acid concentration and that the current paradigm, ascribing fatty acid transport exclusively to FABP may require

modification. Further studies must clarify. But the fatty acid model developed in this report provides a vantage from where future studies can proceed (33-35; 44; 48).

4.6. Conclusion

The ^{1}H NMR analysis reveals that an unsaturated fatty acid, OA, can interact specifically and non-specifically with MbCN. At low OA:Mb, the specific interaction localizes to a structural region neighboring the 8 heme methyl. At high OA:Mb, the non-specific OA interaction disrupts the heme environment. The disruption, however, does not lead to any hemichrome formation. OA solubility increases in the presence of Mb. The OA interaction with Mb does not appear to shift the lamella-micelle equilibrium. Given a fatty acid transport model, Mb appears to compete with FABP above a threshold fatty acid concentration in the cell.

Supplementary Material

Refer to Web version on PubMed Central for supplementary material.

ACKNOWLEDGEMENTS

We gratefully acknowledge funding support from NIH GM 58688 (TJ) and the scientific discussion with and assistance of Dr. Ulrike Kreutzer.

Abbreviations

OA	oleic acid
FABP	fatty acid binding protein
Mb	myoglobin
MbCN	cyanometmyoglobin

Reference

1. Akhrem AA, Andreyuk GM, Kisel MA, Kiselev PA. Hemoglobin conversion to hemichrome under the influence of fatty acids. Biochim Biophys Acta. 1989; 992:191–194. [PubMed: 2503042]
2. Bertini, I.; Luchinat, C.; Parigi, G. Solution NMR of Paramagnetic Molecules. Elsevier; Amsterdam: 2001.
3. Chung Y, Huang SJ, Glabe A, Jue T. Implication of CO inactivation on myoglobin function. Am J Physiol Cell Physiol. 2006; 290:C1616–C1624. [PubMed: 16421206]
4. Chung Y, Jue T. Cellular response to reperfused oxygen in the postischemic myocardium. Am J Physiol. 1996; 271:H687–H695. [PubMed: 8770112]
5. Chung Y, Mole PA, Sailasuta N, Tran TK, Hurd R, Jue T. Control of respiration and bioenergetics during muscle contraction. Am J Physiol Cell Physiol. 2005; 288:C730–C738. [PubMed: 15537712]
6. Cistola DP, Hamilton JA, Jackson D, Small DM. Ionization and phase behavior of fatty acids in water: application of the Gibbs phase rule. Biochemistry. 1988; 27:1881–1888. [PubMed: 3378036]
7. Cistola DP, Small DM, Hamilton JA. Carbon 13 NMR studies of saturated fatty acids bound to bovine serum albumin. I. The filling of individual fatty acid binding sites. J Biol Chem. 1987; 262:10971–10979. [PubMed: 3611099]

8. Cistola DP, Walsh MT, Corey RP, Hamilton JA, Brecher P. Interactions of Oleic-Acid with Liver Fatty-Acid Binding-Protein - A C-13 Nmr-Study. Biochemistry. 1988; 27:711–717. [PubMed: 3349060]
9. Flockhart BD, Graham H. Study of Dilute Aqueous Solutions of Sodium Oleate. J Colloid Sci. 1953; 8:105–111.
10. Flogel U, Laussmann T, Godecke A, Abanador N, Schafers M, Fingas CD, Metzger S, Levkau B, Jacoby C, Schrader J. Lack of myoglobin causes a switch in cardiac substrate selection. Circ Res. 2005; 96:e68–e75. [PubMed: 15817884]
11. Flogel U, Merx MW, Godecke A, Decking UKM, Schrader J. Myoglobin: A scavenger of bioactive NO. Proc Natl Acad Sci. 2001; 98:735–740. [PubMed: 11136228]
12. Fukuda H, Goto A, Yoshioka H, Goto R, Morigaki K, Walde P. Electron Spin Resonance Study of the pH-Induced Transformation of Micelles to Vesicles in an Aqueous Oleic Acid/Oleate System. Langmuir. 2001; 17:4223–4231.
13. Garry DJ, Ordway GA, Lorenz JN, Radford NB, Chin ER, Grange RW, Bassel-Duby R, Williams RS. Mice without myoglobin. Nature. 1998; 395:905–908. [PubMed: 9804424]
14. Glabe A, Chung Y, Xu D, Jue T. Carbon monoxide inhibition of regulatory pathways in myocardium. Am J Physiol. 1998; 274:H2143–H2151. [PubMed: 9841541]
15. Glatz JF, Schaap FG, Binas B, Bonen A, van der Vusse GJ, Luiken JJ. Cytoplasmic fatty acid-binding protein facilitates fatty acid utilization by skeletal muscle. Acta Physiol Scand. 2003; 178:367–371. [PubMed: 12864741]
16. Glatz JF, van der Vusse GJ. Intracellular transport of lipids. Mol Cell Biochem. 1989; 88:37–44. [PubMed: 2674666]
17. Gloster J. Studies on Fatty-Acid Binding Characteristics of Myoglobin and Z-Protein. J Molec Cell Cardiol. 1977; 9:15.
18. Gloster J, Harris P. Fatty-Acid Binding to Cytoplasmic Proteins of Myocardium and Red and White Skeletal-Muscle in Rat - Possible New Role for Myoglobin. Biochem Biophys Res Comm. 1977; 74:506–513. [PubMed: 836303]
19. Godecke A, Flogel U, Zanger K, Ding Z, Hirchenhain J, Decking UK, Schrader J. Disruption of myoglobin in mice induces multiple compensatory mechanisms. Proc Natl Acad Sci U S A. 1999; 96:10495–10500. [PubMed: 10468637]
20. Gotz FM, Hertel M, Groschelstewart U. Fatty-Acid-Binding of Myoglobin Depends on Its Oxygenation. Biological Chemistry Hoppe-Seyler. 1994; 375:387–392. [PubMed: 7980870]
21. Gros G, Wittenberg B, Jue T. Myoglobin's old and new clothes: from molecular structure to function in living cells. J Exp Biol. 2010; 213:2713–2725. [PubMed: 20675540]
22. Hoerr CW, Harwood HJ. The Solubilities of Oleic and Linoleic Acids in Common Organic Solvents. J Phys Chem. 1952; 56:1068–1073.
23. Jansson E, Sylven C. Myoglobin concentration in single type I and type II muscle fibres in man. Histochem. 1983; 78:121–124.
24. Johnson JS, Griffith WL, Compere AL. Small-Angle Neutron-Scattering from Micelles of Potassium-Salts of 18-Carbon Fatty-Acids. Langmuir. 1989; 5:1191–1195.
25. Jung RF, James RO, Healy TW. Adsorption, Precipitation, and Electrokinetic Processes in the Iron-Oxide (Goethite) Oleic-Acid Oleate System. J Colloid Interf Sci. 1987; 118
26. Kanicky JR, Shah DO. Effect of Degree, Type, and Position of Unsaturation on the pKa of Long-Chain Fatty Acids. J Colloid Interf Sci. 2002; 256:201–207.
27. Klevens HB. Structure and Aggregation in Dilute Solutions of Surface Active Agents. J Am Oil Chem Soc. 1953; 30:74–80.
28. Kreutzer U, Jue T. Investigation of bioactive NO-scavenging role of myoglobin in myocardium. Eur J Physiol. 2006; 452:36–42.
29. Kreutzer U, Chung Y, Butler D, Jue T. ^{1}H-NMR characterization of the human myocardium myoglobin and erythrocyte hemoglobin signals. Biochim Biophys Acta. 1993; 1161:33–37. [PubMed: 8422419]
30. Kreutzer U, Jue T. The role of myoglobin as a scavenger of cellular NO in myocardium. Am J Physiol. 2004; 286:H985–H991.

31. La Mar, GN. Model compounds as aids in interpreting NMR spectra of hemoproteins. In: Shulman, RG., editor. Biological Applications of Magnetic Resonance. Academic Press; New York: 1979. p. 305-343.
32. La Mar GN, Davis NL, Parish DW, Smith KM. Heme orientational disorder in reconstituted and native sperm whale myoglobin. J Mol Biol. 1983; 168:887–896. [PubMed: 6887254]
33. Lin PC, Kreutzer U, Jue T. Anisotropy and temperature dependence of myoglobin translational diffusion in myocardium: implication on oxygen transport and cellular architecture. Biophy J. 2007; 92:2608–2620.
34. Lin PC, Kreutzer U, Jue T. Myoglobin translational diffusion in myocardium and its implication on intracellular oxygen transport. J Physiol. 2007; 578:595–603. [PubMed: 17038435]
35. Luxon BA, Weisiger RA. Sex-Differences in Intracellular Fatty-Acid Transport - Role of Cytoplasmic-Binding Proteins. Am J Physiol. 1993; 265:G831–G841. [PubMed: 8238512]
36. Masuda K, Truscott K, Lin PC, Kreutzer U, Chung Y, Sriram R, Jue T. Determination of myoglobin concentration in blood-perfused tissue. Eur J Appl Physiol. 2008; 104:41–48. [PubMed: 18516616]
37. Mendel CM, Mendel DB. 'Non-specific' binding. The problem, and a solution. Biochem J. 1985; 228:269–272. [PubMed: 2988517]
38. Morgan LJ, Ananthapadmanabhan KP, Somasundaran P. Oleate Adsorption on Hematite - Problems and Methods. Int J Min Proc. 1986; 18:139–152.
39. Nakamura Y, Nishida T. Effect of hemoglobin concentration on the oxidation of linoleic acid. J Lipid Res. 1971; 12:149–154. [PubMed: 5554105]
40. Papadopoulos S, Endeward V, Revesz-Walker B, Jurgens KD, Gros G. Radial and longitudinal diffusion of myoglobin in single living heart and skeletal muscle cells. Proc Natl Acad Sci USA. 2001; 98:5904–5909. [PubMed: 11320218]
41. Papadopoulos S, Jurgens KD, Gros G. Diffusion of myoglobin in skeletal muscle cells - dependence on fibre type, contraction and temperature. Pflugers Arch Eur J Physiol. 1995; 430:519–525. [PubMed: 7491278]
42. Ponganis PJ, Kreutzer U, Sailasuta N, Knower T, Hurd R, Jue T. Detection of myoglobin desaturation in Mirounga angustirostris during apnea. Am J Physiol Regul Integr Comp Physiol. 2002; 282:R267–R272. [PubMed: 11742847]
43. Rassaf T, Flogel U, Drexhage C, Hendgen-Cotta U, Kelm M, Schrader J. Nitrite reductase function of deoxymyoglobin: oxygen sensor and regulator of cardiac energetics and function. Circ Res. 2007; 100:1749–1754. [PubMed: 17495223]
44. Richieri GV, Ogata RT, Kleinfeld AM. Equilibrium constants for the binding of fatty acids with fatty acid-binding proteins from adipocyte, intestine, heart, and liver measured with the fluorescent probe ADIFAB. J Biol Chem. 1994; 269:23918–23930. [PubMed: 7929039]
45. Richieri GV, Ogata RT, Kleinfeld AM. Equilibrium-Constants for the Binding of Fatty-Acids with Fatty-Acid-Binding Proteins from Adipocyte, Intestine, Heart, and Liver Measured with the Fluorescent-Probe Adifab. J Biol Chem. 1994; 269:23918–23930. [PubMed: 7929039]
46. Richieri GV, Ogata RT, Kleinfeld AM. The measurement of free fatty acid concentration with the fluorescent probe ADIFAB: A practical guide for the use of the ADIFAB probe. Mol Cell Biochem. 1999; 192
47. Shih L, Chung Y, Sriram R, Jue T. Palmitate interaction with physiological states of myoglobin. Biochim Biophys Acta. 2014; 1840:656–666. [PubMed: 24482816]
48. Sriram R, Kreutzer U, Shih L, Jue T. Interaction of fatty acid with myoglobin. FEBS Lett. 2008; 582:3643–3649. [PubMed: 18840435]
49. Tetko IV, Tanchuk VY, Kasheva TN, Villa AEP. Estimation of aqueous solubility of chemical compounds using E-state indices. J Chem Inf Comp Sci. 2001; 41
50. Tofani L, Feis A, Snoke RE, Berti D, Baglioni P, Smulevich G. Spectroscopic and interfacial properties of myoglobin/surfactant complexes. Biophys J. 2004; 87:1186–1195. [PubMed: 15298921]
51. Tyuzyo K. On the Relation between Viscosity and Critical Micelle Concentration of Detergent Solutions .3. Relations between Micellar Molecular Weight, Viscosity and Critical Micelle Concentration of Detergent Solutions. Bull Chem Soc Japan. 1958; 31

52. Vork MM, Glatz JF, van der Vusse GJ. On the mechanism of long chain fatty acid transport in cardiomyocytes as facilitated by cytoplasmic fatty acid-binding protein. J theor Biol. 1993; 160:207–222. [PubMed: 8474251]

53. Vorum H, Brodersen R, Kraghhansen U, Pedersen AO. Solubility of Long-Chain Fatty-Acids in Phosphate Buffer at Ph-7.4. Biochim Biophys Acta. 1992; 1126

54. White JR. Dissociation Constants of Higher Alkyl Phosphate Esters, Phosphonic Acids, Phosphonous Acids, Phosphinic Acids and Carboxylic Acids. J Am Chem Soc. 1950; 72

55. Wittenberg BA, Wittenberg JB. Transport of oxygen in muscle. Annu Rev Physiol. 1989; 51:857–878. [PubMed: 2653210]

56. Wittenberg JB, Wittenberg BA. Myoglobin function reassessed. J Exp Biol. 2003; 206:2011–2020. [PubMed: 12756283]

57. Zimmels Y, Lin IJ. Stepwise Association Properties of Some Surfactant Aqueous-Solutions. Colloid Polymer Sci. 1974; 252

Highlights

- Oleic acid (OA) interacts specifically and non-specifically with myoglobin.
- At high OA:Mb ratios, the interaction produces a global perturbation of the protein.
- PH titration analysis indicates that Mb does not shift the OA lamella-micelle equilibrium.
- Given the OA interaction with Mb, a fatty acid flux model suggests that Mb can play a role in intracellular fatty acid transport.

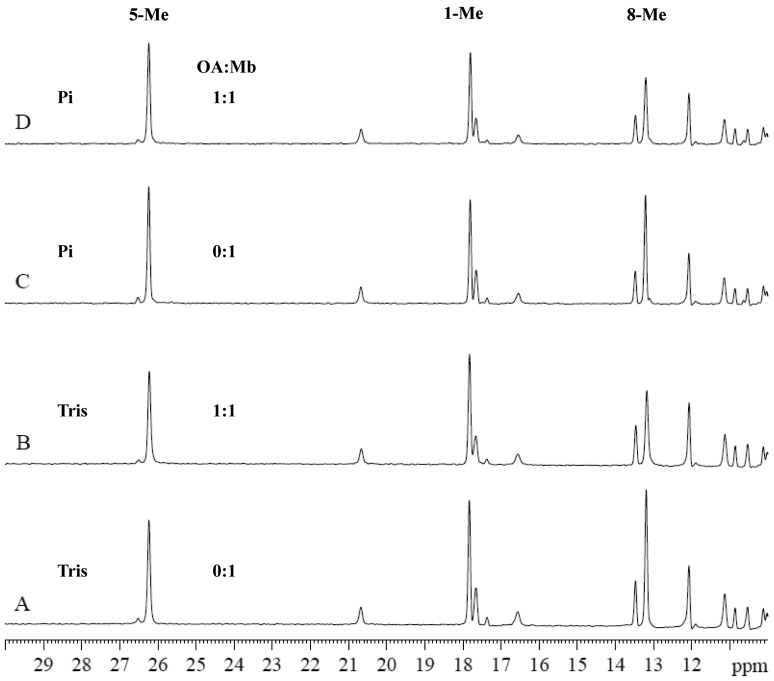

Fig 1.

^{1}H NMR (30-10 ppm) spectra of 0.8 mM MbCN in 30mM Tris or 100mM phosphate buffer with and without OA at pH 7.4 and 35ºC. A) MbCN in 30mM Tris buffer. B) MbCN in 30mM Tris buffer with OA at OA:Mb ratio of 1:1. C) MbCN in 100mM phosphate buffer (Pi) D) MbCN in 100mM Pi with OA at OA:Mb ratio of 1:1. In either Tris or Pi, the heme 5-CH_3 (26.2 ppm) and 1-CH_3 (17.8 ppm) signals show no perturbation with the addition of OA. Only the heme 8-CH_3 signal at 13.2 ppm decreases.

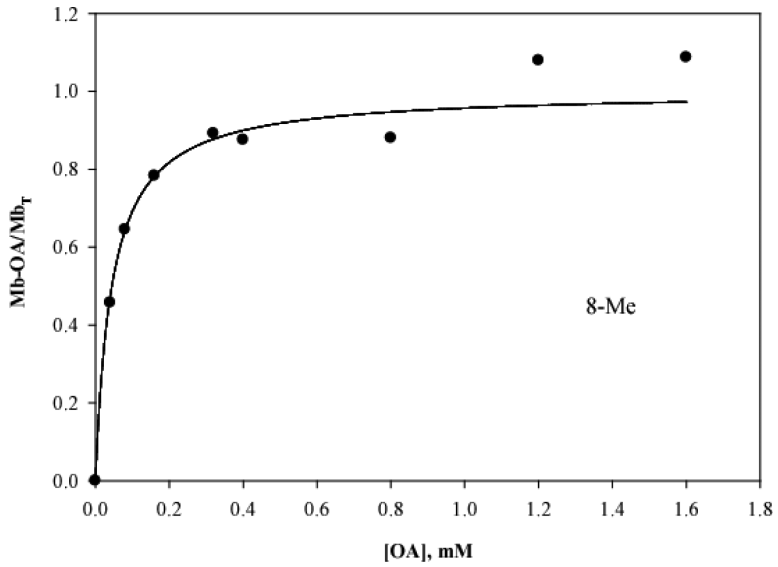

Fig 2.

The fraction of Mb bound to OA (Mb-OA), derived from the assumption that the heme 8-CH_3 peak intensity plateau corresponds to the fully bound Mb-OA state, leads to the determination of an apparent Kd=45 μM.

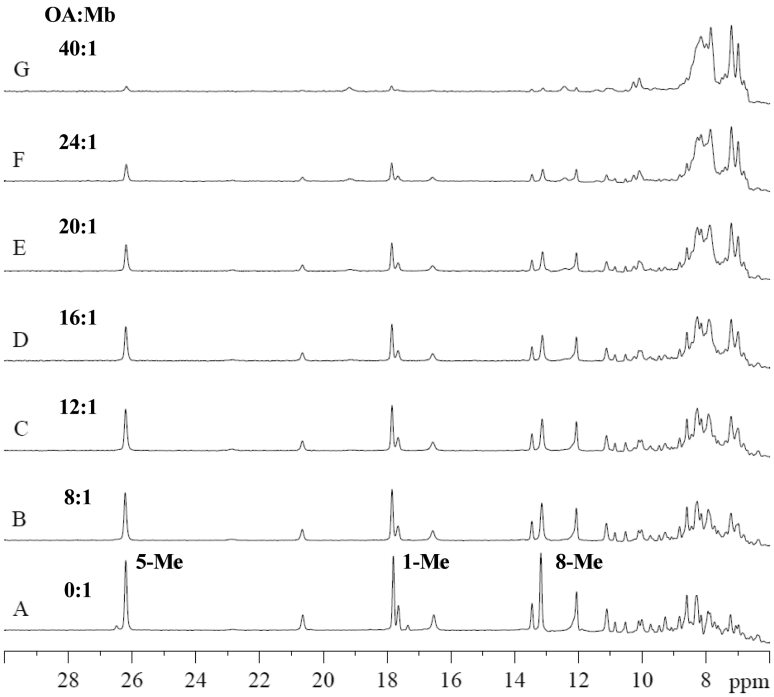

Fig 3.

^{1}H NMR spectra of 0.8 mM MbCN at pH 7.4 and 35ºC during OA titration: A) Control spectrum, OA:MbCN=0 B) OA:MbCN=8:1. C) OA:MbCN=12:1. D) OA:MbCN=16:1. E) OA:MbCN=20:1. F) OA:MbCN=24:1. G) OA:MbCN=40:1.

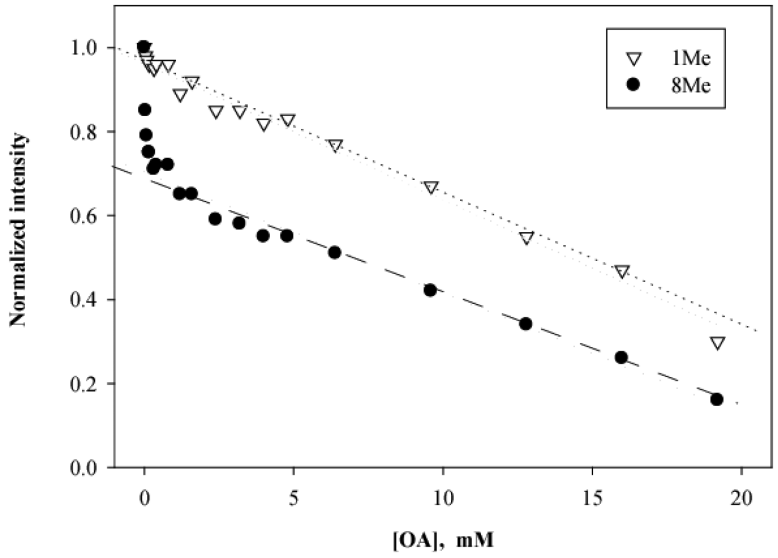

Fig 4.

Graph of heme 1-CH_3 and 8-CH_3 peak intensity of 0.8 mM MbCN at pH 7.4 and 35°C during OA titration: The 8CH_3 peak intensity drops selectively at OA:Mb < 2:1. Above OA:Mb of 2:1, all heme methyl signals and other hyperfine shifted peaks decline. Above the OA:Mb threshold of 24:1, the hyperfine shifted resonances become difficult to quantify. For the heme 8-CH_3 and 1-CH_3, the linear curves from OA:Mb ratio of 2:1 to 20:1 reveal the following relationship: $Y_{8Me} = -0.029x + 0.70$ (r=0.99) $Y_{1Me} = -0.032x + 0.96$ (r=0.99). $Y_{5Me} = Y_{1Me}$ (data not shown).

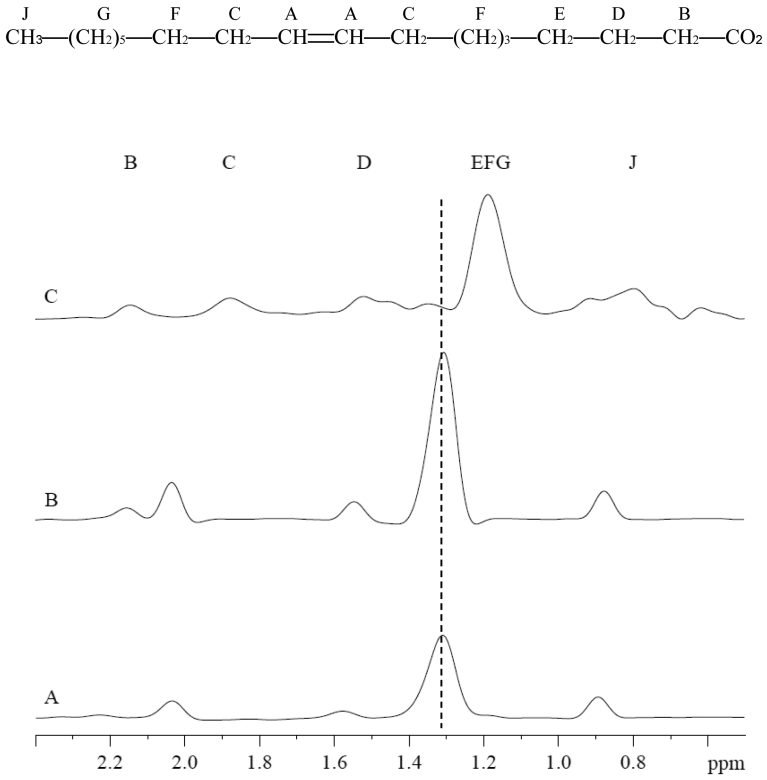

Fig 5.

Comparison of the ^{1}H NMR chemical shifts of 0.8 mM OA in Mb and in Tris at 35ºC: A) in Tris at pH 7.4 B) in Tris at pH 12.1 C) in Mb at pH 7.4 and OA:Mb 1:1. The prominent EFG peaks of OA at pH 7.4 and pH 12.1 have similar chemical shifts. However, in Mb the EFG peak resonates at 1.19 ppm, 0.13 ppm upfield from its chemical shift position in Tris. A similar chemical shift change appears in Pi. Other OA peaks also change in the presence of Mb.

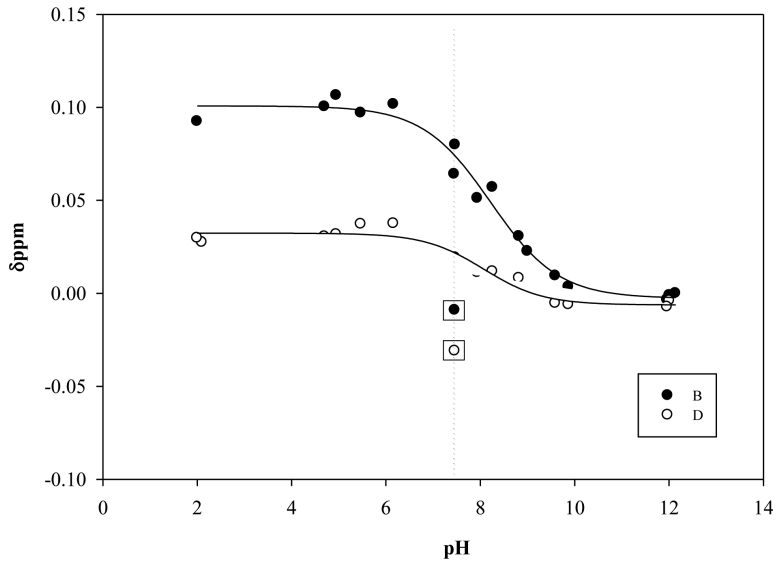

Fig 6.

Graph of the relative pH dependent chemical shift of peaks B and D of OA: The pH titration curve based on the respective chemical shifts referenced to the peak positions at pH 12.14 yields a pK of 8.22 and 8.07 derived from peaks B and D, respectively.

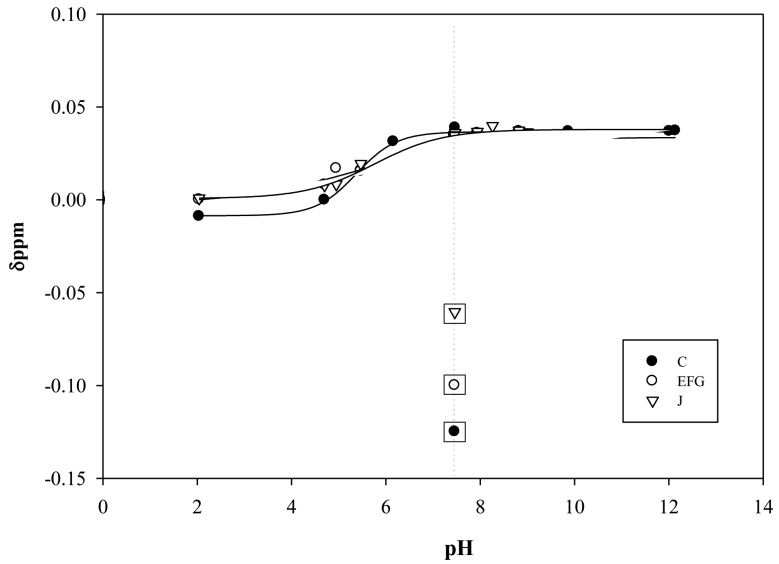

Fig 7.

Graph of the relative pH dependent chemical shift of peaks C, EFG, and J of OA: The pH titration curve based on the chemical shifts referenced to the respective peak positions at pH 2 yields a pK of 5.37, 5.40, and 5.76 respectively derived from peaks C, EFG, and J, respectively.

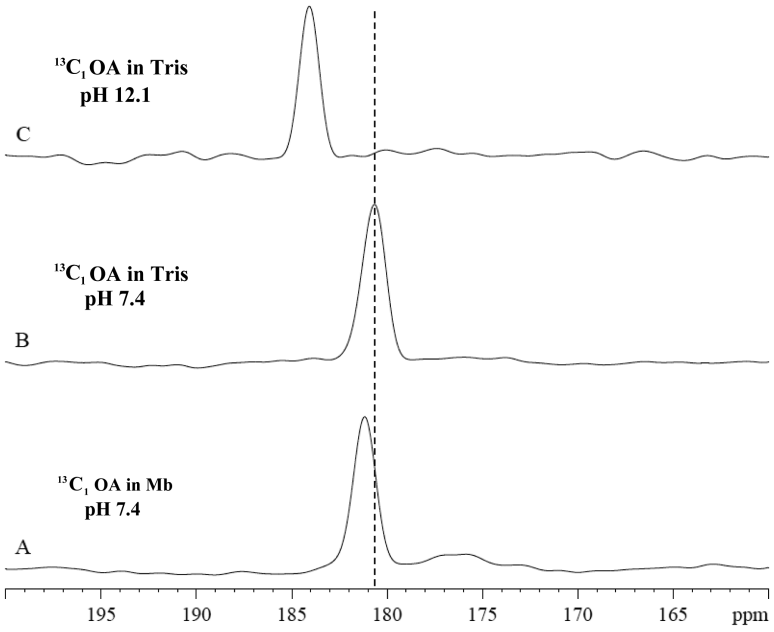

Fig 8.

^{13}C spectra of 0.8 mM $^{13}C_1$ OA at 35°C A) in Mb (181.3 ppm) at pH 7.4 B) in Tris (180.9 ppm) at pH 7.4 and C) in Tris at pH 12.1 (184 ppm).

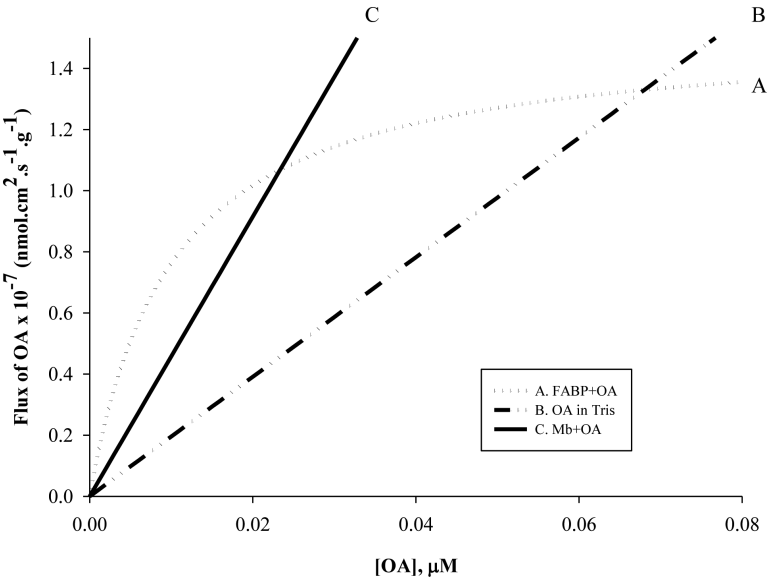

Fig 9.

Model of cellular fatty acid flux with curves corresponding to A) OA bound to 50uM FABP with Kd=10nM. B) OA in Tris (43% solubility) C) OA bound to 260 μM Mb with an apparent Kd=45 μM. Diffusion coefficients listed in Table 6. Mb-OA flux exceeds FABP-OA flux at at OA concentration exceeding 0.02μM, and free fatty acid flux in Tris buffer exceeds FABP-OA flux at OA concentration above 0.07 μM.

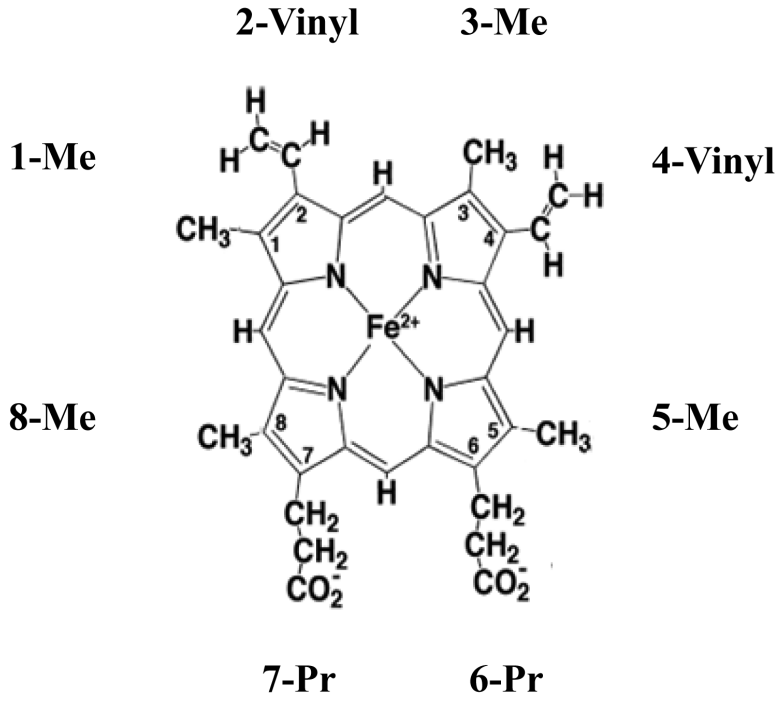

Inset Figure.

Table 1

Chemical Shift of Oleic Acid Peaks

	^{13}C NMR OA Chemical Shift ppm		**^{1}H NMR OA Chemical Shift ppm**				
	$-CO_2$	**A**	**B**	**C**	**D**	**EFG**	**J**
[1]$CDCl_3$	180.6	5.34	2.27	2.03	1.59	1.27-1.35	0.90
[2]Tris, pH 7.4	180.9	ND	2.23	2.11	1.58	1.32	0.90
[2]Tris, pH 12	184.0	ND	2.16	2.04	1.55	1.31	0.88
[2]MbCN, pH 7.4 [2]pK	181.3	ND	2.15 8.22	1.88 5.37	1.53 8.07	1.19 5.41	0.79 5.76

ND = not detectable. Peak A of oleic acid in chloroform appears at 5.34 ppm.

[1]No. 1035, Spectral Database for Organic Compounds (SDBS), SDBSWeb : http://sdbs.db.aist.go.jp (National Institute of Advanced Industrial Science and Technology).

[2]This work

Table 2

Linewidth of Oleic Acid Peaks

	^{13}C NMR OA Linewidth Hz	^{1}H NMR OA Linewidth Hz				
pH	**$-CO_2$**	**B**	**C**	**D**	**EFG**	**J**
Tris pH 7.4	209 ± 11	49 ± 7	38 ± 3	49 ± 2	49 ± 1	37 ± 1
Tris pH 12.1	183 ± 3	35 ± 1	35 ± 1	39 ± 1	49 ± 1	35 ± 1
MbCN pH 7.4	203 ± 4	46 ± 3	46 ± 3	45 ± 2	60 ± 5	59 ± 3

Table 3

Oleate solubility

Solution	Solubility M	Solubility g/100g	Reference
[1]0.8mM MbCN in Tris, pH 7.4 35°C	2.49×10^{-3}	7.03×10^{-2}	This work
[1]10.8mM MbCN in phosphate, pH 7.4 35°C	2.33×10^{-3}	6.59×10^{-2}	This work
[1]30 mM Tris buffer, pH 7.4 35°C	1.43×10^{-3}	4.04×10^{-2}	This work
[1]30 mM Tris buffer, pH 12 35°C	2.99×10^{-3}	8.45×10^{-2}	This work
[1]100 mM phosphate buffer, pH 7.4 35°C	1.26×10^{-3}	3.56×10^{-2}	This work
Water at 20-25°C	$4.28\text{-}44.0\times10^{-7}$	$1.21\text{-}12.4\times10^{-5}$	(38; 49)
0.2 M HEPES, pH 7.4 at 37°C	6.00×10^{-6}	1.70×10^{-4}	(46)
66 mM phosphate buffer, pH 7.4 at 37°C	1.00×10^{-6}	2.83×10^{-5}	(53)
Acetone at 20°C	∞	∞	(22)
Benzene at 20°C	∞	∞	(22)
95% of ethanol at 20°C	∞	∞	(22)

[1]Defined at 3.2mM or 0.0904g/100g of total OA added.

Table 4

Oleic acid pK

OA mM	pK	Temp °C	Method	Reference
[1] 0.8-3.2 mM	8.42	35	^{13}C NMR	This work
[2] 0.8 mM	8.07-8.22	35	^{1}H NMR	This work
[3] 0.8 mM	5.37-5.76	35	^{1}H NMR	This work
1-2 mM	5.02	25	neutralization endpoint	(54)
10 mM	4.95	25	surface tension	(25)
80 mM	8-8.5	39	^{13}C NMR	(8)
25 mM	8-9	25	ESR	(12)
350 mM	9.85	20	neutralization endpoint	(26)

[1] pK determined from the ^{13}C chemical shift of C_1 OA during pH titration.

[2] pK determined from the ^{1}H chemical shifts of B and D during pH titration: Peak B yields a pK=8.22, whereas peak D yields a pK=8.07.

[3] pK determined from the ^{1}H chemical shifts of peak C=5.37, EFG=5.41, and J=5.76.

Table 5

Critical micelle concentration (CMC) of Oleic Acid

CMC mM	Temperature °C	Method	Reference
0.8	25	refraction	(27)
0.9	25	small angle neutron scattering	(24)
0.9-1	25	dye titration	(27)
1	20	viscosity	(51)
1.1	40	small angle neutron scattering	(24)
[1]2.1	26	conductivity	(57)
2.1	25	conductivity	(9)

Oleate, the conjugate base of oleic acid, would form micelles in the aqueous solution. The critical micelle concentration (CMC) values of oleate were measured in the pure water.

[2]SANS stands for small angle neutron scattering.

[1]The pH is measured as 10.3.

Table 6

Fatty acid flux model parameters

Parameter		Value	Reference
Concentration, (μM)	FABP (C_{FABP})	50	(52)
	Mb (C_{Mb})	200-500	(23; 36; 56)
Dissociation Constant (μM)	$^{1}K_{Mb1}$	45	This Work
	KMb2	37×10^{3}	This Work
	K_{FABP}	1.4×10^{-2}	(15; 45).
Diffusion Constant (D, cm^2s^{-1})	Fatty acid (D_{OA})	4.6×10^{-6}	(52)
	FABP (D_{FABP})	3.05×10^{-9}	(35)
	Myoglobin (D_{Mb})	7.85×10^{-7}	(34)
Equipoise [OA] at Flux A= Flux B (μM)	Mb & FABP	0.02	This Work
	OA in Mb & FABP	0.03	This Work
	OA in Tris & FABP	0.07	This Work
Maximum Facilitated Fatty Acid Flux ($nmolcm^2s^{-1}g^{-1}$)	Mb in Mammalian Muscle	$1.6\text{-}3.9 \times 10^{-4}$	This Work
	FABP	1.5×10^{-7}	This Work
DC/K (cm^2s^{-1})	Mb	3.72×10^{-6}	This Work
	FABP	1.53×10^{-5}	This Work
OA Solubility (M)**	Tris	4.3×10^{-1}	(48)
	MbCN	8.2×10^{-1}	This Work

K_{Mb1} = specific binding; K_{Mb2} = non-specific binding